

A CONTAMINANT ICE VISUALIZATION EXPERIMENT IN A GLASS PULSE TUBE

J. L. Hall and R. G. Ross, Jr.

Jet Propulsion Laboratory
California Institute of Technology
Pasadena, CA 91109

A. K. Le

Department of Chemical Engineering
UCLA
Los Angeles, CA 90095

ABSTRACT

Results are presented from pulse tube experiments designed to investigate the effect of 400 parts per million water vapour contaminant of helium working gas. The experiments were conducted in a glass pulse tube to enable visualization of ice formation on internal surfaces. Photographs of this ice formation were taken along with simultaneous cold tip temperature and compressor power measurements. Four different types of regenerator elements were tested in various combinations: 200 and 400 mesh stainless steel screen, 1.6 mm diameter glass beads, and 1.6 mm thick perforated plastic plate. Internal spacers were also used to provide clear fields of view into the regenerator stack. Substantial water-ice formation was observed at the cold end of the regenerator and on the inside wall of pulse tube, often becoming visible within half an hour of operation. The regenerator ice appeared to be highly porous like snow and was seen to accumulate only in a very thin region at the cold end despite changing the cold tip temperature across a range of 150 to 235 K. Ice formation degraded pulse tube thermal performance only in cases where screen was used at the regenerator cold end and good wall contact was established on the circumference. It was concluded that flow blockage was the mechanism by which

contaminants affected performance, so that coarse regenerator elements were largely immune over the tested time scale of a few days. Substantially reduced ice formation and minimal performance loss were also observed in repeated tests where the contaminated gas was reused after warming up and melting the accumulated internal ice. Substantial adsorption of the liquid water onto the regenerator was inferred, a process that depleted the gas phase concentration of water. The addition to the regenerator of water adsorbing zeolite or saran carbon material did not noticeably improve this adsorption process.

INTRODUCTION

Gas phase contaminants inside pulse tube cryocoolers will freeze at sufficiently low operating temperatures. If enough frozen material accumulates, there will be a loss of overall thermal performance due to one or more possible mechanisms such as flow blockage, internal geometry change or increased parasitic heat conduction. The source of these contaminants can be either impurities in the helium charge gas or outgassing of internal cooler surfaces over time. Both sources are typically present in actual systems with the relative importance a function of gas purity, cleaning procedures, materials of construction and seal performance.¹ A recent investigation² focused on the charge gas impurity aspect of the problem and found modest performance losses due to water, carbon dioxide, argon and nitrogen contaminants at levels ranging from 10 to 100 ppm per component. The observed performance loss occurred over a time scale of approximately 1 week, a value which was estimated to be the gas diffusion time scale inside the pulse tube used for those experiments. Before and after measurements with a mass spectrometer did not reveal any appreciable accumulation of contaminants due to outgassing of internal surfaces over the 1 week test period.

One of the limitations of the previous investigation was the lack of visual observations of contaminant ice formation inside the metal pulse tube. Thermal performance loss was determined from temperature and power consumption measurements, but it was not possible to deduce where the ice was forming or what specific physical mechanism was responsible for the performance loss. The present investigation was designed to address this problem by conducting experiments in a glass pulse tube that allowed direct observation of internal ice formation. The overriding intent was to enhance the visualization aspect of the experiment at the cost of refrigeration performance. In practice, the use of a glass tube and the absence of multilayer insulation limited the cold tip temperatures to 150 K as opposed to the 60 K temperatures achieved in the earlier study.

EXPERIMENTAL APPARATUS

The experiments were performed with a simple orifice pulse tube mounted on a Lockheed two piston back-to-back linear compressor (Fig. 1). The compressor had a maximum swept volume of 5.0 cm³ (2.5 cm³ per piston). The pulse tube consisted of a quartz glass tube with stainless steel end connections at the top and bottom. The glass to metal interfaces consisted of flared, grooved joints that were clamped together and sealed with standard rubber O-rings. The glass tube was comprised of two sections, a 19 mm O.D. lower part that housed the regenerator, and a 10 mm O.D. upper part that was the pulse tube itself. The two tubes were fused together to form a smooth shoulder joint. The nominal glass thickness was 1.6 mm. An

"L"-shaped copper busbar was used to thermally connect the orifice end of the pulse tube to the cooled reservoir plate. Indium shims placed between the copper bus bar and the top of the pulse tube served the dual purpose of improving the junction heat transfer and increasing the mechanical pre-load on the stack to enhance the compression, and hence performance, of the glass to metal O-ring seals.

The system was typically operated in the range of 36 to 40 Hz with no applied heat load and a fixed heat rejection temperature of 0 °C. The heat rejection temperature was maintained by a chiller unit circulating an ethylene glycol and water mixture through the pulse tube mounting plate. A gas pressure of 1.5 MPa (200 psig) was used in all tests. Two different gas compositions were employed: a "clean" gas comprised of five-nines pure helium, and a "contaminated" gas comprised of helium with 400 ppm of water vapor. The corresponding partial pressure of water at this concentration and pressure is 4 torr, which in turn, corresponds to a vaporization temperature of 275 K.³ The compressor was operated open-loop using an HP 3325B function generator and a Techron 7540 power amplifier to provide a sinusoidal power input. An LVDT sensor mounted on each compressor piston provided position data that was plotted in real time on an oscilloscope. Manual control of the power amplifier was used to set the piston stroke as indicated on the oscilloscope.

Temperature data was provided by Lakeshore DT 470 cryodiodes bonded onto the outside of the glass tube at 3 locations (Fig. 1). The middle location, just below the shoulder joint, was defined to be the "cold tip" temperature for these experiments. For most of the experiments, the temperature data was recorded every minute on a portable PC computer using National Instruments LabView data acquisition software. Compressor input power was measured by a Valhalla 2300L Programmable Three-phase Digital Power Analyzer.

Two different vacuum enclosures were used for these experiments. Initially, a small acrylic cylinder was bolted onto the pulse tube base plate (Fig. 2) and sealed with a Viton O-ring. This arrangement provided good optical access; however, outgassing of the acrylic limited the achievable vacuum levels to approximately 3×10^{-5} torr. This limitation became unacceptable once pulse tube cold tip temperatures of approximately 205 K or less were achieved because residual water vapour began to freeze on the outside of the pulse tube and obscured the internal view. The addition of a crude liquid nitrogen cryopump to the acrylic chamber succeeded in lowering the vacuum level to 1×10^{-6} torr, but this was still not sufficient to prevent external frost at the lowest cold tip temperatures. Therefore, some tests were conducted with the entire pulse tube placed in a 0.45 m diameter glass bell jar. A combination of a 1-stage Gifford-McMahon cryopump and mechanical drag pumps succeeded in generating vacuum levels as low as 6×10^{-7} torr, sufficient to prevent all external icing. However, the glass bell jar was not constructed of optical quality glass and this degraded our ability to take high quality visual observations and photographs during those tests.

Visual inspection of the tests was enhanced by use of a Zeiss binocular microscope. This device provided an effective magnification of approximately 3 at standoff distances of up to 0.5 m. Photographs were taken with a hand-held 35 mm single lens reflex camera employing a 50 mm lens and 200 ASA print film. To obtain a focus at close range (~10 cm), the camera lens was mounted on 45 mm of standoff tubes. Adequate depth of field was achieved by stopping the camera down to f/16 or f/22. One or two tungsten halogen lamps were used to provide illumination for the pictures with typical exposure times of 1/60 seconds or less.

Four different kinds of regenerator elements were tested in various combinations. These were: 1.6 mm glass beads; perforated 1.6 mm thick acrylic plates with typically 30% porosity

and 1.6 mm holes; 200 mesh stainless steel screen; and 400 mesh stainless steel screen. The glass beads and perforated plates were primarily used to provide better visual access to the inside of the regenerator stack. An experiment with a particular regenerator and gas composition lasted anywhere from a few hours to a week. Every time the pulse tube was opened up to change the regenerator, the inside surface was cleaned with a propanol-soaked Kimwipe tissue. After re-assembling the pulse tube, it would be internally evacuated at room temperature with a turbopump for one to three days to remove the air. Although the residual contamination was not measured, our previous experience² suggests that a level of 20-30 ppm of residual water and nitrogen is achieved with this kind of cleaning.

RESULTS AND DISCUSSION

A total of 30 pulse tube tests were conducted in this study to explore contamination effects in the different regenerators across a cold tip temperature range of 150 K to 235 K. Several of these tests were done with clean helium gas to establish a proper baseline performance at various temperatures. Many photographs were taken during these experiments to document the extent of internal ice formation. Eight photographs have been included in this paper to illustrate the key findings. They are presented in Figures 3 through 6, arranged in pairs from 4 different experiments. Although the regenerators and cold tip temperatures were different in each test, all used the same 400 ppm water contaminated helium gas. Figure 3 shows a double perforated plate over glass bead regenerator both before the start of the experiment and after one day of continuous operation at 235 K. Note the use of small glass columns to separate the plates and provide a clear view of the entire plate surface. Figure 4 shows a perforated plate over 200 mesh stainless steel screen regenerator before the start and after 2 days of continuous operation. Figure 5 shows a 200 mesh stainless steel screen regenerator after 1 day and after 6 days of continuous operation. Figure 6 shows a regenerator with 50 layers of 400 mesh screens on top of 200 mesh screens after 1 day and 4 days of continuous operation.

Perhaps the most significant result illustrated by these photographs is that every experiment with fresh 400 ppm water contaminated helium gas produced enough internal frost formation to be visible to the naked eye. In general this frost became visible on the inside wall of the small diameter tube section above the regenerator within half an hour of starting the pulse tube. Figures 5a, 6a, and 6b show this wall frost after it had accumulated for one or more days. It took longer (2+ hours) to see frost accumulating on regenerator surfaces, presumably because of the greater difficulty of seeing it in those locations rather than because of smaller accumulation rates. Interestingly enough, the frost always accumulated on the top surface of regenerator elements, and even then only on those elements at the very top of the stack. For example, both plates in Fig. 3b show frost on the top surface, while corresponding oblique views from below (not shown) revealed no frost underneath. A few of the glass beads right below the second plate also showed frost deposits, but no frost is seen lower down the stack. A similar pattern is seen in Fig. 4, where only the plate and the top one or two layers of screen show frost accumulation. In Fig. 5a and 5b we see frost only on the top screen and not in the gap that was left 10 screen layers below the top. No counter-examples were seen to this pattern of frost accumulation occurring only at the very top of the regenerator stack despite achieving cold tip temperatures as low as 150 K in some tests.

The frost that collects on the regenerator is highly porous like snow. This is seen most clearly in Fig. 6a in which there is literally a pile of tiny ice shards stacked up on the center of the screen. These ice shards were only seen in this experiment and its repeat. In every other case, magnified microscope observations indicated that the frost tended to build up as a large number of thin tendrils side by side, very much like the frost that forms on an exposed liquid nitrogen pipe in air. Over time these tendrils merged to form more jumbled patches like in Figs. 4b and 6b. The ice shard pile in Fig. 6a also disappeared in time and became the more uniform coating seen in Fig. 6b. Despite the fact that this porous "snow" accumulated on only the top of exposed surfaces, it was never observed to fall downwards. As far as our observations could determine, the frost structures only grew by accretion of gas phase material.

Another result illustrated by the photographs is the tendency of the internal frost to redistribute itself over time. For example, the tube wall frost in Fig. 5a has disappeared five days later in Fig. 5b. Also, the fairly uniform coating on the screen in Fig. 5a has developed some bare patches over the same time period. The disappearance of the ice shard pile from Fig. 6a to Fig. 6b is another example of this redistribution. However, it should be stressed that at lower temperatures, namely below 200 K, there generally seemed to be less redistribution of frost over the same few day time scale.

Time traces of cold tip temperature from six different experiments are presented as Figs. 7a through 7f. The first four correspond in sequence to the tests whose photographs are shown in Figs. 3 through 6. Figure 7e shows data from the lowest temperature experiment in this study, while Fig. 7f compares the data from 7d with a repeat experiment at the same test conditions. All of the plots show temperature spikes at irregular intervals. This is due to the high power camera lamps that were used to illuminate the pulse tube for photography and microscopy. The radiative heat transfer from these lamps was clearly large compared to the nominal parasitic heat load on the uninsulated glass pulse tube. Another feature seen in Figs. 7a, b, d and f is a regular temperature oscillation with an amplitude of 1 K or less. The cause this oscillation is not known; however, it is speculated to be a result of temperature fluctuations in the ethylene glycol and water chiller unit that removes heat from the pulse tube.

All of these time traces come from experiments where the compressor piston stroke and heat rejection temperature set point were held constant. Therefore, any change in the mean cold tip temperature can be attributed to internal contamination effects. The data indicate quite strongly that internal frost formation did not necessarily correspond with thermal performance loss. For example, the mean temperature in Figs. 7a and 7b is constant with time despite the large accumulations of frost as seen in the corresponding photographs in Figs. 3 and 4. This constancy was mirrored by compressor power measurements taken at the same time. Conversely, the mean temperature in Figs. 7c and 7d is not constant with time. In Fig. 7c, the mean temperature rises approximately 5 K by mid-experiment, only to decay back to the original value by the sixth day. A similar pattern is seen in Fig. 7d in which there is an initial temperature rise from 213 K to 217 within the first few hours, then a slow decay down to 215 K by the end of the experiment. These temperature movements generally coincided with the internal frost redistributions illustrated in the photographs, namely the formation of a bare spot on the screen in Fig. 5b and the disappearance of the ice shard pile in Fig. 6a. Experiments at lower temperature that featured much less internal frost redistribution showed correspondingly less temperature recovery. For example, a 155 K all-screen regenerator result is shown in Fig. 7e. After a partial temperature recovery at the half-day mark, the temperature climbed back again to a value roughly 5 K higher than the start value.

Evaluation of all the temperature and frost data revealed that cold tip temperatures changed only in experiments using screen regenerators that were pushed up against the shoulder joint at the pulse tube – regenerator tube junction. All tests with spacers or plates at the shoulder joint showed no change of temperature with time. The conclusion we draw from this is that the mechanism by which frost degrades the overall thermal performance is flow blockage, and that only small pore regenerator elements (like screens) that have excellent circumferential contact are susceptible to this blockage. Large pore elements like perforated plates or beads, and elements that do not form very small gaps at the glass wall junction, were not sufficiently blocked by internal frost formation. The corollary to this conclusion is that poor contact at the outer edge of screens or other small pore elements will allow enough flow at the wall to mitigate the blockage of the pores themselves. This suggests that the use of small spacers at the top of any pulse tube regenerator can alleviate much of the blockage effect by allowing for the flow to slide around the circumference and away from the frosted center.

A handful of tests were conducted in which pairs of experiments were performed under identical conditions with the same 400 ppm water contaminated helium gas. The gas was allowed to heat back up to room temperature between tests, but was not replaced or otherwise processed. During the warming process, it was generally observed that all of the accumulated ice inside the pulse tube melted in the range of 275 to 280 K, forming visible water drops that typically evaporated over the course of a few hours. The striking results from the repeat experiments were significantly less frost formation and negligible cold tip temperature change. Fig. 7f shows time traces from one such repeated experiment in which it appears that the first experiment used contaminated gas and the second used clean gas, even though the gas was not replaced between experiments. We speculate that the water drops that form during the warm-up phase between experiments wet the surface of the regenerator screens to such an extent that a significant amount became physically adsorbed, thereby depleting the gas phase concentration of water. In addition, the time scale for desorption of this water must have been longer than the few day duration of the subsequent experiment in order for it not to reappear as visible frost. The large surface area of a screen regenerator coupled with a vast number of small crevices formed by wire to wire contact would seem to promote both physical adsorption and capillary condensation mechanisms; however, no detailed analysis has yet been performed to evaluate the plausibility of this adsorption theory for the apparent disappearance of gas phase water between experiments.

The dramatic effect of water drop adsorption onto regenerator screens suggested the possibility of adding specific adsorption elements to the regenerator to enhance the process. Two kinds of adsorbants were tested: a zeolite (molecular sieve) in 1.6 mm diameter bead form, and saran carbon in large pellet form. The zeolite was located near the high temperature end of the regenerator, while the saran carbon was placed near the cold temperature end. In neither case, however, was frost reduction observed using fresh gas. Time traces of cold tip temperature likewise revealed no change due to blockage. One experiment was performed with a second saran carbon pellet placed at the top of the pulse tube on the possibility that significant water was reaching the cold tip from the downstream reservoir; however, this change also had no effect on the observed frost formation. A repeat experiment with the same gas after warmup showed the same behaviour as regenerators without saran carbon, namely apparent depletion of gas phase water and much reduced frost formation.

The reasons for the zeolite and saran carbon null result are not clear. It is possible that the surface area of the zeolite and saran carbon was too small to adsorb water at the necessary

rate. Both may also have been limited by the vacuum bakeout temperature of only 100 °C that was achievable with this configuration. Nevertheless, this null result is surprising and will require future work to properly understand.

CONCLUSIONS

Glass pulse tube experiments were conducted with four different kinds of regenerator elements. Substantial internal ice formation was observed when 400 ppm water contaminated helium gas was tested across a cold tip temperature range of 150 to 235 K. The ice formation was limited to a thin region at the coldest end of the regenerator in all tests. The ice appeared to be highly porous like snow and was observed to redistribute itself over time, especially in the tests above 205 K. Internal ice formation only degraded pulse tube thermal performance in tests using screen elements at the regenerator cold end with good tube wall contact. Experiments with coarse regenerator elements or spacers at the end of the regenerator seemed immune to the blockage-induced performance degradation. Experiments in which water contaminated gas was reused after warmup and melting of accumulated ice showed significantly reduced ice formation and negligible performance loss. It was concluded that substantial adsorption had occurred of the liquid water onto the regenerator surfaces, thus depleting the gas phase concentration of water.

ACKNOWLEDGEMENTS

The work described in this paper was carried out at the Jet Propulsion Laboratory, California Institute of Technology and was jointly sponsored by the Caltech President's Fund and the NASA EOS IMAS TechDemo Project through an agreement with the National Aeronautics and Space Administration. The authors would like to acknowledge the laboratory assistance of Scott Leland at JPL.

REFERENCES

- ¹ Getmanets, V. F. and Zhun, G. G. "Cryocooler Working Medium Influence on Outgassing Rate", presented at the 10th International Cryocooler Conference, Monterey, CA, 26-28 May, 1998.
- ² Hall, J. L. and Ross, R. G. Jr. "Gas Contamination Effects on Pulse Tube Performance", presented at the 10th International Cryocooler Conference, Monterey, CA, 26-28 May, 1998.
- ³ O'Hanlon, J. F., *A User's Guide to Vacuum Technology*, John Wiley & Sons, N.Y., 1980, p 364.

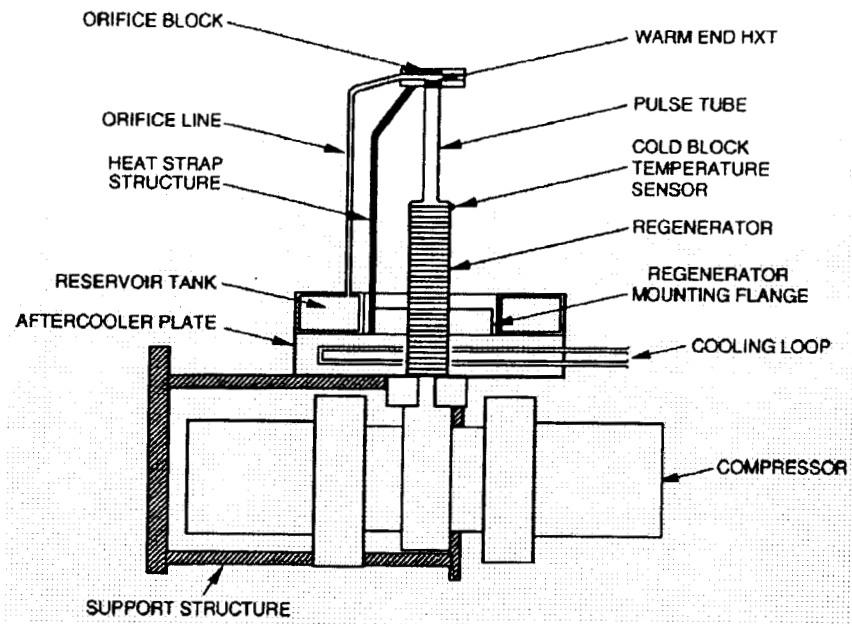


Fig. 1: Schematic Diagram of Glass Pulse Tube

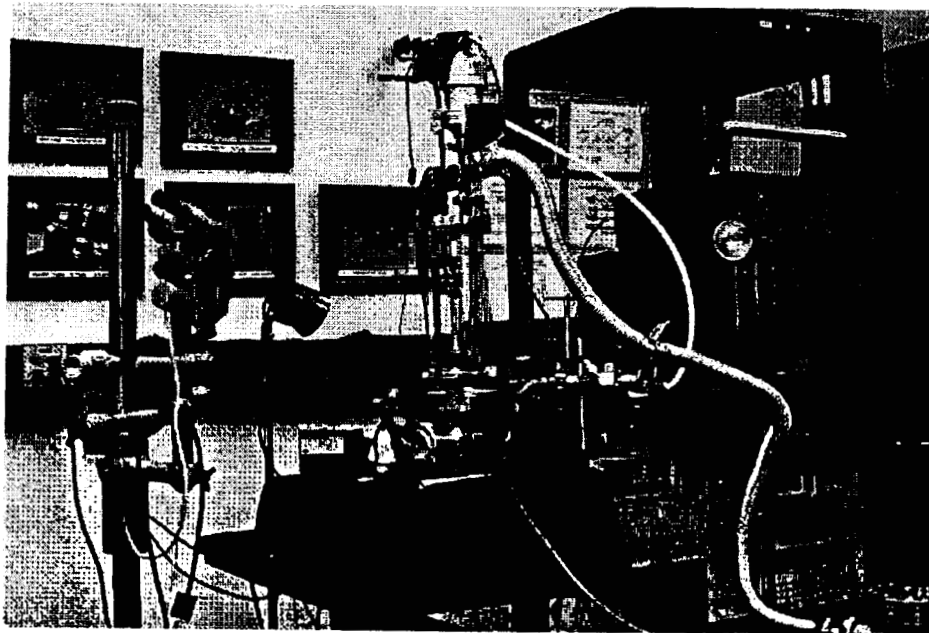


Fig. 2: Photograph of Glass Pulse Tube in an Acrylic Vacuum Enclosure



(a)



(b)

Fig. 3: Photographs of double-plate over glass bead regenerator, before and after icing (GPT 5).

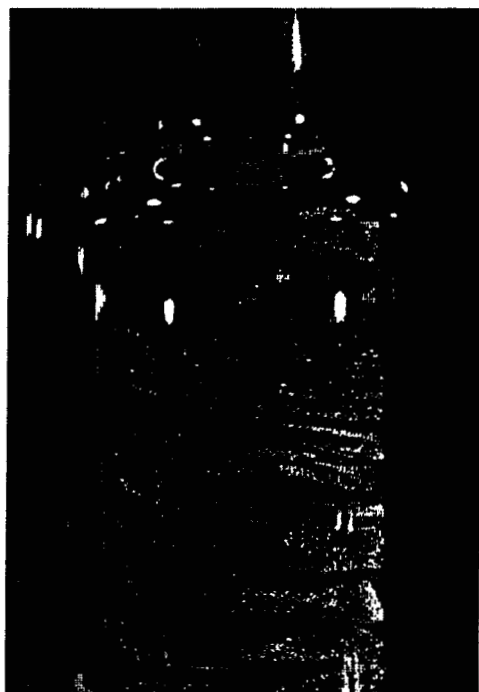


(a)

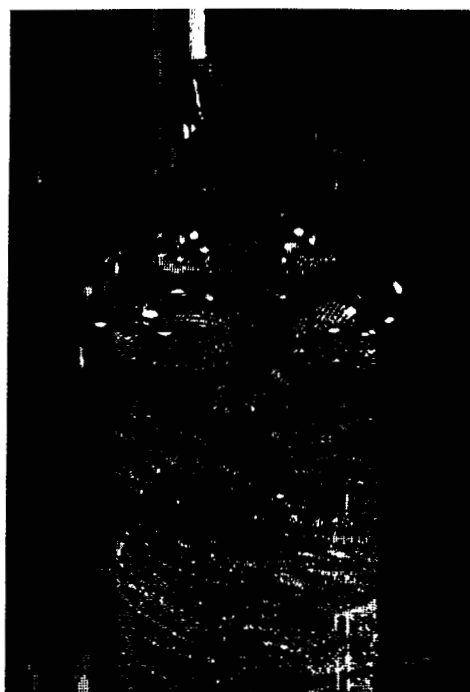


(b)

Fig. 4: Photographs of plate over 200 mesh screen regenerator, before and after icing (GPT 9).



(a)



(b)

Fig. 5: Photographs of screen regenerator with spacer below shoulder joint, after 1 day and after 6 days of continuous operation (GPT 10).



(a)



(b)

Fig. 6: Photographs of all screen regenerator after 1 day and 4 days of operation (GPT 16).

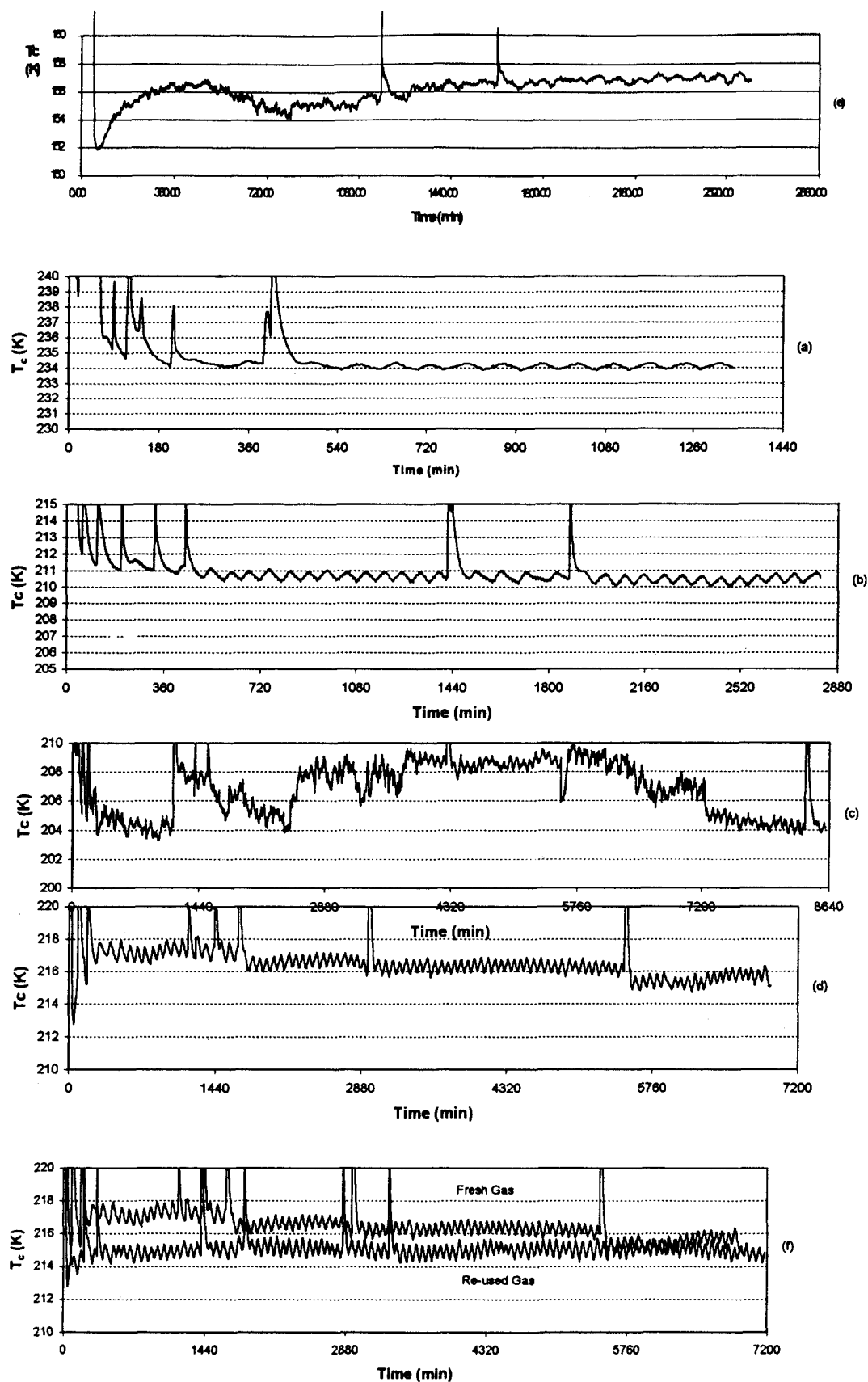


Fig. 7: Cold block temperature vs time traces for selected experiments.